CHAPTER 31

DECOMPOSITION OF NONLINEARLY REFLECTED IRREGULAR WAVES BY THE WAVE BREAKING AND DEFORMATION

by A. KIMURA*

ABSTRACT

This paper deals with a new method to decompose incident and reflected waves from the measured data of irregular standing waves. The theory by Goda et al. is extended to cope with the reflection from such a coastal structure that has a sloping surface and brings about different reflection coefficient for each incident waves. Irregular standing waves are decomposed into incident and reflected irregular waves by the short-term wave spectrum analysis method. And the reflection coefficient of the approximated zero-up-cross waves are defined as the ratio between envelopes of these irregular wave profiles. The calculated reflection coefficients can be discussed in terms of the incident zero-up-cross wave parameters such as a wave steepness, Ursell parameter, etc. An effective wave gauge system to measure irregular standing waves which have a wide band spectrum is also discussed and a method to compose the system is proposed.

1. INTRODUCTION

The theories by Kajima[1], Thornton et al.[2] and Goda et al.[3] have been commonly used to decompose incident and reflected waves from irregular standing waves formed in the vicinity of a model of off-shore structure. With these theories, irregular wave data measured at two or more different points[1] in a wave tank are firstly analyzed by the Fourier transform method and then decomposed into incident and reflected waves. The reflection coefficient is calculated for every frequency component of a spectrum. By these methods reliable reflection coefficients are calculated from an experiment of irregular waves when incident and reflected waves η_I and η_R can be written in the form

* Associate Prof. Faculty of Engg. Tottori University, Koyama Minami 4-101, Torrori, 680, Japan

$$\eta_I(t)=\sum_{n=1}^{\infty} a_{In}\cos(2\pi f_n t-\phi_{In}) \tag{1}$$

and

$$\eta_R(t)=\sum_{n=1}^{\infty} a_{Rn}\cos(2\pi f_n t-\phi_{Rn}) \tag{2}$$

in which f_n is the frequency of the n-th component. a_{In}, a_{Rn} are the amplitudes, ϕ_{In}, ϕ_{Rn} are the phases of incident and reflected waves, respectively.

In case of a breakwater made of stones or blocks, which has a sloped surface, however, the reflection characteristics of the irregular waves change almost wave by wave which are defined by the zero-up-cross method. A wave with a large steepness, for example, tends to break on a slope and loses significant part of its energy. Therefore, the resultant reflection coefficient is presumably very small for this wave. On the contrary, a wave with a small steepness is reflected with a large reflection coefficient, since it may not break on the slope. Since reflection coefficients differ wave by wave for this type of breakwater, amplitudes and phases in eq.(2) may change occasionally. There has been no established method to calculate the amplitude and phase of each wave from those reflected irregular waves. The amplitudes and phases of component waves decomposed by the ordinary Fourier transform method are, therefore, apparent ones in the analysis of reflection for this type of breakwaters. A large portion of existing offshore structures, however, somehow exhibit this type of reflection.

This study aims to develop a method which facilitates the calculation of the reflection coefficient of irregular waves reflected from this type of breakwater.

2. DECOMPOSITION OF IRREGULAR STANDING WAVES INTO INCIDENT AND REFLECTED COMPONENT WAVES

For simplicity, the reflection of uni-directional irregular waves from a breakwater is treated in this study (see Fig.1). The coordinate system is shown in the same figure. Wave gauges with the interval $\Delta\ell$ are installed at a distance D from the breakwater. This breakwater is assumed to be of such a type that changes reflection characteristics according to the individual incident wave properties (e.g. steepness). Amplitudes and phases of reflected component waves in eq.(2), therefore, may be assumed constant only within a zero-up-cross interval of the wave profile. The Fourier transform method requires the constant amplitudes and phases of component waves. However, since they are disturbed locally, data are analyzed with a data window in this study.

$$\gamma(u)=(\sqrt{2}/T')\exp[-\pi(t-u)^2/T'^2] \tag{3}$$

This window is the so called Gaussian window and has finite values only around t=u and has negligibly small values outside $t=u\pm T'/2$. Executing the convolution with wave profiles $\eta_1(t)$ and $\eta_2(t)$ measured at $x=x_1$ and $x=x_2$ in the wave tank respectively and the data window, amplitude of composed (i.e., incident and reflected) component wave is given as

$$A_{jn}(u)+iB_{jn}(u)=\frac{2}{T}\int_{-T/2}^{T/2}\eta_j(t)\gamma(u)\exp(-i2\pi f_n t)dt \tag{4}$$

in which $i=\sqrt{-1}$, $T\gg T'$, $f_n=n/T$ (n=1,2,...) and $A_{jn}(u)$ and $B_{jn}(u)$ are

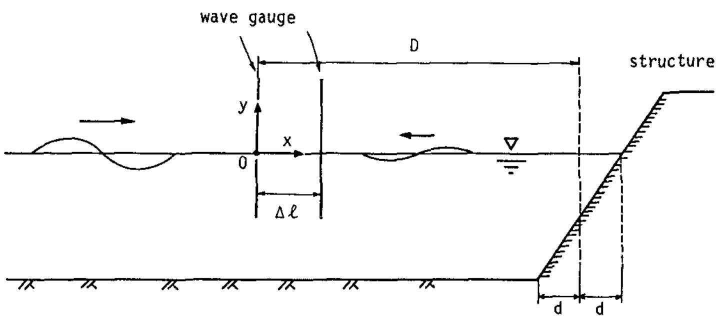

Fig.1 Illustration of wave gauges and a structure and the coordinate system.

real and imaginary parts of the n-th Fourier component of a spectrum. Subscript j indicates that those are the calculated values from the wave profiles $\eta_j(u)$ (j=1,2). Substituting these components into the following equations, amplitudes and phases of incident and reflected component waves are obtained[3]:

$$a_{In}(u)=\frac{1}{2|\sin(k_n\Delta\ell)|}\{[A_{2n}(u)-A_{1n}(u)\cos(k_n\Delta\ell)-B_{1n}(u)\sin(k_n\Delta\ell)]^2$$
$$+[B_{2n}(u)+A_{1n}(u)\sin(k_n\Delta\ell)-B_{1n}(u)\cos(k_n\Delta\ell)]^2\}^{1/2}$$

$$a_{Rn}(u)=\frac{1}{2|\sin(k_n\Delta\ell)|}\{[A_{2n}(u)-A_{1n}(u)\cos(k_n\Delta\ell)+B_{1n}(u)\sin(k_n\Delta\ell)]^2$$
$$+[B_{2n}(u)-A_{1n}(u)\sin(k_n\Delta\ell)-B_{1n}(u)\cos(k_n\Delta\ell)]^2\}^{1/2}$$

$$\phi_{In}(u)= \tan^{-1}\left[\frac{-A_{2n}(u)+A_{1n}(u)\cos(k_n\Delta\ell)+B_{1n}(u)\sin(k_n\Delta\ell)}{B_{2n}(u)+A_{1n}(u)\sin(k_n\Delta\ell)-B_{1n}(u)\cos(k_n\Delta\ell)}\right] - k_n x_1$$

$$\phi_{Rn}(u)= \tan^{-1}\left[\frac{-A_{2n}(u)+A_{1n}(u)\cos(k_n\Delta\ell)-B_{1n}(u)\sin(k_n\Delta\ell)}{-B_{2n}(u)+A_{1n}(u)\sin(k_n\Delta\ell)+B_{1n}(u)\cos(k_n\Delta\ell)}\right] - k_n x_1 \tag{6}$$

in which $a_{In}(u)$ and $a_{Rn}(u)$ are amplitudes and $\phi_{In}(u)$ and $\phi_{Rn}(u)$ are phases of incident and reflected component waves. Wave number k_n has the following relation with f_n:

$$(2\pi f_n)^2 = g k_n \tanh(k_n h) \tag{7}$$

in which h is a water depth and g is the acceleration of gravity. Figure 2 shows an example of decomposed incident and reflected irregular wave components $a_{In}(u)$ (above) and $a_{Rn}(u)$ (below). Analyzed irregular waves are numerically simulated for the spectrum given by eq.8.

$$S(f)=2^{1/4}\exp[-\pi(f-f_p)^2\tau^2] \tag{8}$$

In which the peak frequency f_p and the width parameter τ are 1.0Hz and 5s respectively. One hundred component waves from f=0.84Hz to 1.16Hz are composed in the simulation. The reflection coefficient of the breakwater is set to be 0.5 and no phase shift is assumed at the breakwater for all the component waves. Other parameters such as h=10cm, $\Delta\ell$ =23cm (1/4 wave length of the dominant component, f_n=1.0Hz), D=(2+0.23)m and T'=5s (eq.3) are used in the calculation. Plotted are the amplitudes of dominant frequency (f_n=1.0Hz).
Gradual changes of the incident and reflected wave amplitudes are

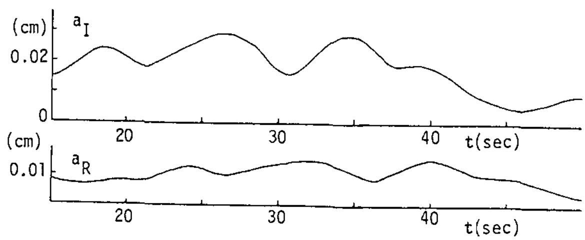

Fig.2 Gradual change in decomposed amplitudes of incident and reflected waves (f_n=1.0Hz).

observed in Fig.2. Only a time-independent single couple of incident and reflected amplitudes for individual component waves are obtained from the ordinary theories. The gradual changes in the present method are due to the leakage of a data window. The data window works not only for the emphasis of local property of data but also for the reduction of a resolution power by the Fourier transform method. If $\cos(2\pi f_0 t)$, for example, is analyzed instead of $\eta_j(t)$ in eq.(4), the calculated Fourier spectrum is not a single spike spectrum but has a spreading of spectrum values around $f=f_0$ as shown in Fig.3. This broad nature of the calculated spectrum is so called the leakage of a spectrum. The neighboring frequency components bring about this gradual change in the amplitudes (Fig.2). These changes in a_{In} and a_{Rn} are not the independent and random ones but seem to be coherent with each other since the prominent peaks in a_{In} reappear in a_{Rn} with some time interval. Although amplitude of reflected peaks reduce somehow. The averaged interval between these corresponding peaks is about 5.5s and this is the time required to go back and forth over the distance D (see Fig.1), with a group velocity of the dominant component wave (f_n=1.0Hz). The ratios between the time shifted amplitude $a_{Rn}(u-5.5)$ and the incident amplitude $a_{In}(u)$ are approximately 0.5 at any time irrespective of u. The gradual changes in the calculated wave amplitudes due to leakage, therefore, may be considered as an advantage of this method for the study of local correspondences of incident and reflected waves inspection.

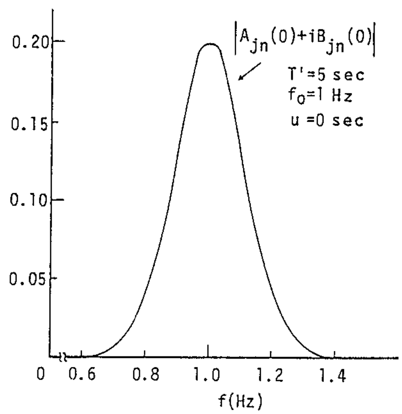

Fig.3 Leakage of a calculated spectrum.

3. THE METHOD OF EVALUATING THE LOCAL REFLECTION COEFFICIENT FROM THE ENVELOPES

Incident wave profile $\eta_I(u)$ and its envelope $E_I(u)$ are given in terms of $a_{In}(u)$ and $\phi_{In}(u)$ as

$$\eta_I(u)=\sum_{n=1}^{\infty} a_{In}(u)\cos[-2\pi f_n u+\phi_{In}(u)] \tag{9}$$

and

$$E_I(u)=[\eta_{Ic}^2(u)+\eta_{Is}^2(u)]^{1/2} \tag{10}$$

where

$$\eta_{Ic}(u)=\sum_{n=1}^{\infty} a_{In}(u)\cos[-2\pi(f_n-f_p)u+\phi_{In}(u)]$$

$$\eta_{Is}(u)=\sum_{n=1}^{\infty} a_{In}(u)\sin[-2\pi(f_n-f_p)u+\phi_{In}(u)] \tag{11}$$

Reflected wave profile $\eta_R(u)$ and its envelope E_R are also expressed in terms of $a_{Rn}(u)$ and $\phi_{Rn}(u)$ in the same way as

$$\eta_R(u)=\sum_{n=1}^{\infty} a_{Rn}(u)\cos[-2\pi f_n u+\phi_{Rn}(u)] \tag{12}$$

and

$$E_R(u)=[\eta_{Rc}^2(u)+\eta_{Rs}^2(u)]^{1/2} \tag{13}$$

where

$$\eta_{Rc}(u)=\sum_{n=1}^{\infty} a_{Rn}(u)\cos[-2\pi(f_n-f_p)u+\phi_{Rn}(u)]$$

$$\eta_{Rs}(u)=\sum_{n=1}^{\infty} a_{Rn}(u)\sin[-2\pi(f_n-f_p)u+\phi_{Rn}(u)] \tag{14}$$

Solid lines in Fig.4 show $\eta_I(u)$ (above) and $\eta_R(u)$ (below). Dotted lines are envelopes $E_I(u)$ and $E_R(u)$. Analyzed irregular waves are the same as those used in the calculation of Fig.2.
Numerically simulated incident waves and their calculated reflection waves are composed first and then decomposed into incident and reflected wave profiles again by use of equations from eqs.(4) to (6) and eqs.(9) to (14). Calculated decomposed wave profiles of incident and reflected waves show good agreements with those originally simulated ones.

Figure 5 shows the Lissajous' figure of E_I and E_R although E_R is shifted by 5.5s to adjust a time correspondence with E_I. The solid line shows the relation of E_R=0.5E_I. Since the reflection coefficient is set to be 0.5, this is approximately the theoretical relation in this case. Except small deviations in the small part, the agreement is found fairy good.
The present method is extended to evaluate the reflection coefficient of individual waves defined by the zero-up-cross method in terms of their properties (e.g. steepness) as follows. Since E_I and E_R approximately pass the crests and troughs of waves as seen in Fig.4 and from the

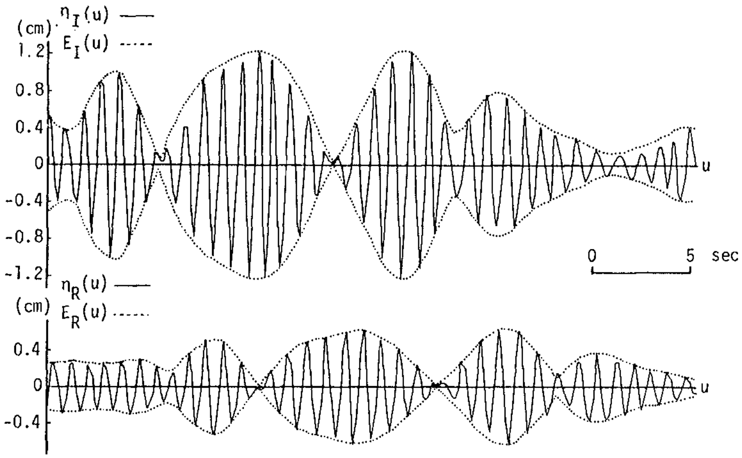

Fig.4 Decomposed wave profiles (solid lines) and their envelopes (dotted lines) for narrow-band spectrum case.

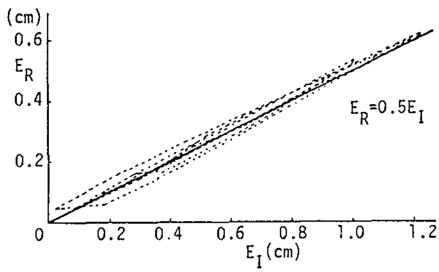

Fig.5 Lissajous' figure of E_I and E_R.

definition that an envelope is symmetrical about the u-axis, wave envelope may presumably have an instance u_i, within a zero-up-cross interval, when the twice of the envelope is equal to the zero-up-cross wave height determined in the same interval. Incident and reflected wave heights $H_I(u_i)$ and $H_R(u_i)$ are, therefore, approximated by equations

$$H_I(u_i) \simeq 2E_I(u_i), \qquad H_R(u_i) \simeq 2E_R(u_i) \tag{15}$$

The wave period of individual waves are approximated as follows. Equation 4 gives the short-term wave spectrum[4] in terms of u. The squared sum of amplitudes $|A_{jn}{}^2+B_{jn}{}^2|$ then changes from time to time according to the local properties of waves. The occasional zero-up-cross wave period can be approximated with $1/f_p(u_i)$ in which $f_p(u_i)$ is the peak frequency of the above squared spectrum at the instance u_i when the wave height is determined by eq.(15). The wave length is approximated by the small amplitude wave theory with this $1/f_p(u_i)$[5]. The wave steepness, for example, is determined as

$$H_I/L_I|_{t=u_i} \simeq 2E_I(u_i)/L_I[f_p(u_i)] \tag{16}$$

where $L_I[f_p(u_i)]$ is the wave length given by

$$L_I[f_p(u_i)] = \frac{g}{2\pi f_p^2(u_i)} \tanh \frac{2\pi h}{L_I[f_p(u_i)]} \tag{17}$$

The reflection coefficient at the instance is therefore given as

$$r(u_i) = 2E_R\{u_i - 2D/C_g[f_p(u_i)]\}/2E_I(u_i) \tag{18}$$

in which $C_g[f_p(u_i)]$ is the group velocity of a frequency $f_p(u_i)$. As explained so far, the present theory uses wave envelopes instead of wave heights to calculate the reflection coefficients. Because the reflection coefficients calculated from the corresponding wave profiles may inevitably include errors to a certain degree due to a dispersive nature of irregular wave profiles. The change in the envelope, on the other hand, is rather gradual and small in comparison with the irregular wave profile itself unless the distance is large.[6] So the present method may have an advantage in the calculation of reflection coefficients. However a clear definition of the instance u_i to determine wave height and frequency (period) in eqs.(15) - (18) still has not been developed.

4. ARRANGEMENT OF WAVE GAUGES FOR THE MEASUREMENT OF IRREGULAR WAVES OF A WIDE BAND SPECTRUM

The fundamental concept of the present theory is exemplified for a irregular waves of narrow band spectrum in the former chapter. The theory is verified for irregular waves of a wide band spectrum in this chapter. In case of a wide band spectrum, there are component waves which make $\sin(k_n\Delta\ell)$ equal or nearly equal to 0 in the denominator of eqs.(5) and (6). Calculated reflection coefficients for these component waves are extremely inaccurate. The theory by Goda et al.[3] recommended an interval from $0.1\pi/k_n$ to $0.9\pi/k_n$ as an effective frequency or wave number range where reliable reflection coefficients can be calculated with eqs.(5) and (6). In this connection, a little narrower range from $0.3\pi/k_n$ to $0.7\pi/k_n$, for example, should be employed to improve the resolution. The narrower the effective frequency range becomes, however, the wider the incalculable frequency range becomes in the spectrum. To avoid this situation, the multi-wave gauge system is adopted in this study. Wave gauges are arrayed irregularly so that there is at least one suitable wave gauge pair that guarantees an effective frequency range for all the component waves in the spectrum. Intervals of wave gauges are determined as follows, if the same effective frequency range as above mentioned is adopted. The largest wave gauge interval $\Delta\ell_1$ is calculated in terms of the given low frequency bound f_d to be analyzed in the spectrum as

$$\Delta\ell_1 = \frac{0.3}{2} L(f_d) \tag{19}$$

in which $L(f_d)$ is the corresponding wave length of f_d. An upper bound of the effective frequency range f_1 for this pair of wave gauges is determined implicitly by

$$\Delta\ell_1 = \frac{0.7}{2} L(f_1) \tag{20}$$

The second largest wave gauge interval $\Delta\ell_2$ is given as

$$\Delta\ell_2 = \frac{0.3}{2} L(f_1) \tag{21}$$

since f_1 should be the lower bound of the effective frequency range for the second interval, if no overlapping of effective frequency ranges is permitted. Repeating the same procedures from eq.(19) to eq.(21) until the upper frequency bound for the i-th wave gauge interval f_i (i=1,2,...) exceeds the high frequency bound f_u to be analyzed in the spectrum, whole intervals of the system ($\Delta\ell_i$) (i=1,2,...) can be determined. Intervals of a sample wave gauge system is listed in Table-1. Pierson-Moskowitz spectrum whose peak frequency f_p equals to 1.0Hz is used in a calculation of these intervals. High and low frequency bounds of the spectrum are set to be 0.5Hz and 3.5Hz, respectively, effective frequency interval is set to be $0.3\pi \leq k_n < 0.7\pi$ and water depth h is set to be 10cm.

Four pairs of wave gauges are necessary to cover the entire frequency range in this case. Example arrangements of wave gauges in this case are schematically shown in Fig.6 (a), (b) and (c). The direction of incident wave is from left to right. Centers of all pairs of wave gauges coincide with each other in the system (a), one wave gauge is commonly used as a partner of the individual pairs in the system (b) and some wave gauges are commonly used twice as a partner in two wave gauge pairs in the system (c). A total number of wave gauges can be reduced in the system

Table-1 Sample of the wave gauge intervals and their effective frequency range.

f(Hz)	0.50-1.09	1.09-2.02	2.02-3.18	3.18-3.50
$\Delta\ell$(cm)	29.2	12.5	5.4	2.3

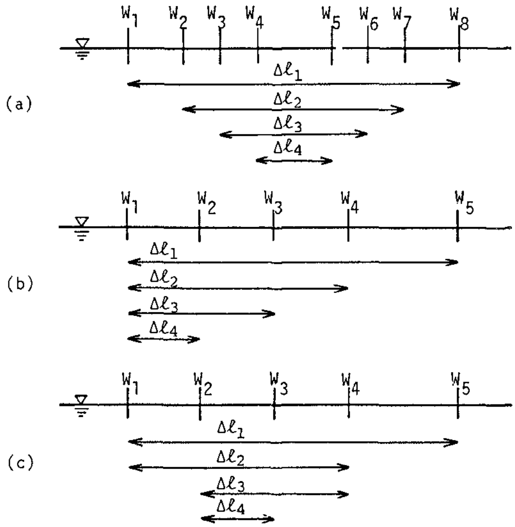

Fig.6 Samples of the wave gauge system.

(b) and (c). Judging from the numerical simulation, the resolution by the system (c) is preferable to (b). The origin of x-axis in the system (c) is preferable to set on the offshore-side a wave gauge pair which is used to analyze the dominant component. And the system is preferable to apply as close as possible to the structure.

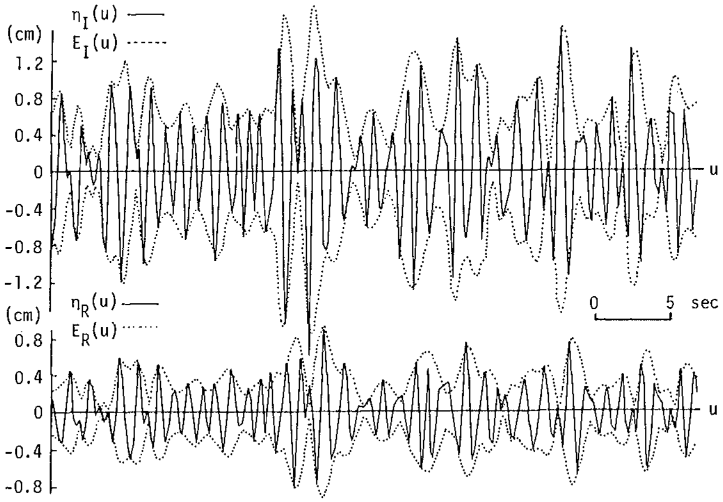

Fig.7 Decomposed wave profiles (solid lines) and their envelopes (dotted lines) for wide-band spectrum case.

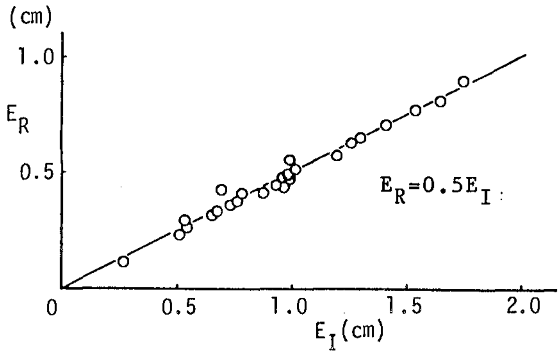

Fig.8 Relation of the values at the prominent summits in the wave envelopes for incident and reflected wave profiles.

Figure 7 shows the calculated result of incident and reflected wave profiles and their envelopes by the system (c). The distance from W-1 to the breakwater is set to be 0.3m. The reflection coefficient is set to be 0.5 and no phase is shifted for all the component waves. Notations and lines are the same as those used in Fig.4. Local disagreements between wave profiles and envelopes are a little prominent in comparison with the narrow band spectrum case. This comes from the asymmetric nature of the wave profile with the zero-level line, which irregular waves with a wide band spectrum usually have. With the ordinary method which dispenses with a data window[7], however, calculated results are almost the same as those by the present method. It can be distinguished from this figure and has been sometimes reported in the field measurements that irregular waves tend to form groups in a few waves which are enveloped by a single prominence of an envelope. Despite of the remarkable changes between incident and reflected wave profiles, the wave envelope maintains its form even after the reflection and transition. And every calculated time interval between the corresponding summits in the envelopes is almost equal to that required to go back and forth over the distance D with the group velocity of the wave around the summit. Every wave group presumably behaves as a single wave "packet[8]" in the process of reflection and transition. At the trough of an envelope, the side foot of the neighboring packets cross each other. Then the Lissajous' figure of E_R and E_I shows inevitably fluctuations around their troughs. To minimize this error, reflection coefficients are calculated only at the summit of individual prominences in E_R and E_I in

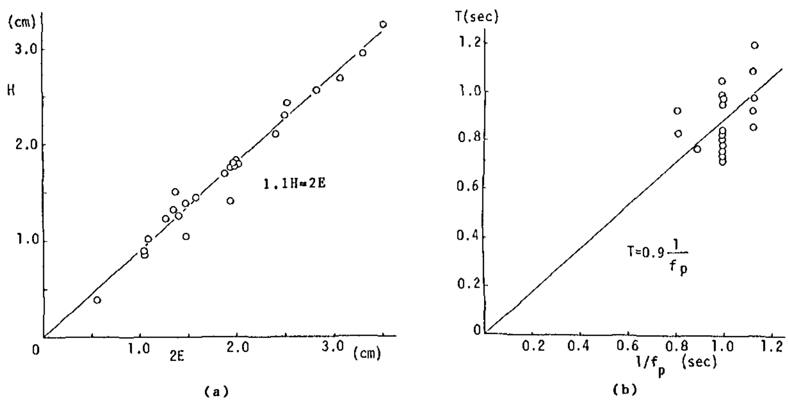

Fig.9 Comparison of (a) wave height, (b) wave period between those by the zero-up-cross method and the present definition.

this study. The relations of corresponding summits in E_I and E_R in Fig.7 are plotted in Fig.8. The solid line shows the relation of $E_R=0.5E_I$. The reliable reflection coefficient can be evaluated for those values. Wave height and period (frequency) in eqs.(15) - (17) are, then, determined at the prominent summit of the envelope. The calculated wave heights and periods, however, tend to be a little larger in this theory than those determined by the zero-up-cross method.

Figure 9 (a) shows the relation between the wave height determined by eq.(15) at the prominent summit of the envelopes and that by the zero-up-cross method just around the same instance. The solid line shows the relation $1.1H_I=2E_I$ or $1.1H_R=2E_R$. Figure (b) shows a relation of the zero-up-cross wave period to $1/f_p(u_i)$ at the prominent summit of an envelope. The solid line shows the relation of $T=0.9/f_p(u_i)$. Although the data show a little scattering, the zero-up-cross wave height and period can be approximated with the small modifications for calculated wave height and period. The calculated reflection coefficient from the present theory, therefore, can be discussed in terms of local properties of incident waves such as the steepness, Ursell number, etc. The numerically calculated constants for modifications, i.e., 1.1 and 0.9 in Fig.9 (a) and (b) respectively, are almost the same as those for wide band spectra such as Pierson-Moskowitz, Neumann and JONSWAP spectrum.

5. DISCUSSION

Since we assumed that an amplitude and a phase of a reflected wave may be constant only within a zero-up-cross interval, the width parameter of the data window in eq.(3) is desirable to be of the same order as that for a period of the dominant wave. The smaller this value becomes, however, the more uneven characteristics of the wave envelope prevail and the wider the calculated reflection coefficients fluctuate on the average. On the contrary, the larger this value becomes, the more locally the occasional nature of wave properties are averaged. Since the single wave group consists of 2-5 waves with similar properties (i.e., wave height, wave period) on the average, reflection characteristics of waves around the summit of an envelope may be assumed mutually equal. Two to five times of the dominant wave period is recommended for this value.

REFERENCES

1) Kajima, R: Estimation of an incident wave spectrum under the influence of reflection, Proc. 13th IAHR, Vol.5-1, pp.285-287, 1969.
2) Thornton, E. B. and R. J., Calhoun: Spectral resolution of breakwater reflected waves, Proc. ASCE, Vol.98, WW4, pp.443-460, 1972.
3) Goda, Y., Y. Suzuki, Y. Kishira and O. Kikuchi: Estimation of incident and reflected waves in random wave experiments, Tec. Note of P.H.R.I.M.T., No.248, 24p., 1976. (in Japanese)
4) Mark, W. D.: Spectral analysis of the convolution and filtering of non-stationary stochastic process, J. Sound Vib., Vol.11, No.1, pp.19-63, 1970.
5) Kimura, A. and Y. Iwagaki: wave length, wave velocity and shoaling characteristic of random waves, Proc. 16th ICCE, pp.320-339, 1978.
6) Kimura, A., H. Hokimoto and A. Seyama: Transition of wave groups Rept. of Faculty of Engg. Tottori Univ., Vol.14, No.1, pp.235-245, 1983. (in Japanese)
7) Rice, S. O.: Mathematical analysis of random noise, Selected papers on noise and stochastic processes, Dover, pp.133-294, 1954.
8) Kinsman, B.: Wind waves, Prentice-Hall, 1945.